J. Fluid Mech. (1982), *vol.* 117, *pp.* 171–185
Printed in Great Britain

Stability of a vortex street of finite vortices

By P. G. SAFFMAN AND J. C. SCHATZMAN
Applied Mathematics, California Institute of Technology,
Pasadena, CA 91125, U.S.A.

(Received 2 April 1981 and in revised form 1 September 1981)

The stability of the finite-area Kármán 'vortex street' to two-dimensional disturbances is determined. It is shown that for vortices of finite size there exists a finite range of spacing ratio κ for which the array is stable to infinitesimal disturbances. As the vortex size approaches zero, the range narrows to zero width about the classical von Kármán value of 0·281.

1. Introduction

The Kármán vortex street is a regular pattern of vortices consisting of two parallel staggered rows, which, for a certain range of Reynolds number, is observed in the wake of two-dimensional blunt bodies placed in a uniform stream. In a previous paper (Saffman & Schatzman 1981) an inviscid model for the wake flow was described which consists of two rows of staggered vortices of finite size, extending to infinity in both directions. Steady solutions (which propagate relative to the free stream) were found numerically, and their properties were calculated. These describe an infinite array of uniform two-dimensional vortices, consisting of one row of identical vortices of area A and strength $-\Gamma$ with centroids at positions $x = 0, \pm l, \pm 2l, \pm 3l, \ldots, y = 0$, and of a second row of identical vortices of area A and strength $+\Gamma$ with centroids at $x = d, d \pm l, d \pm 2l, d \pm 3l, \ldots, y = -h$. The frame of reference is chosen with a uniform flow U_s in the x-direction at infinity as in figure 1 so that the vortices are stationary. It is assumed that the flow is inviscid, incompressible, two-dimensional, and, outside the vortices, irrotational. The case $\mu \equiv d/l = 0{\cdot}5$ was mainly considered (for values of μ other than 0 and 0·5 translating solutions exist but the street does not move parallel to itself; see Rosenhead (1929)). There are then two independent dimensionless parameters $h/l \equiv \kappa$ and $A/l^2 \equiv \alpha$ which determine the geometry of the street.

This paper discusses the stability of these steady solutions to two-dimensional disturbances. A normal-mode analysis is carried out and the growth rates and frequencies of the modes are calculated for a range of values of the vortex size and separation/spacing ratio of the street. It is found that finite size can stabilize the street to infinitesimal disturbances. The results for superharmonic disturbances are in accord with those predicted by energy arguments based on Kelvin's variational principle. It will be pointed out that a plausible but non-rigorous attempt to use these energy arguments for subharmonic disturbances leads to fallacious conclusions.

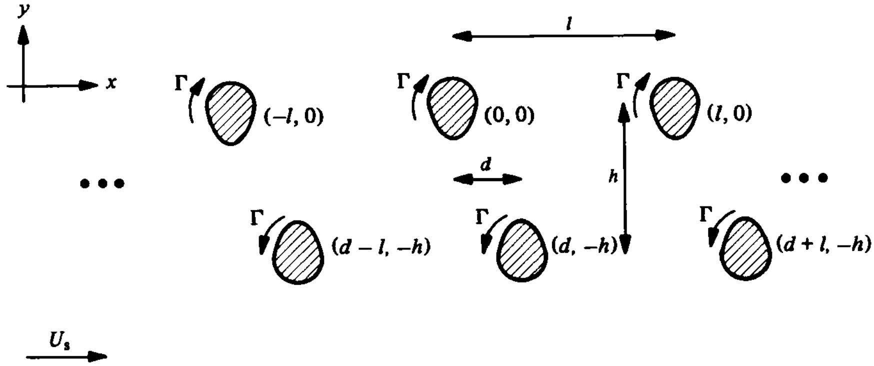

FIGURE 1. The configuration of the fully infinite vortex street with arbitrary stagger.

2. Subharmonic Instabilities of the point-vortex array

The limiting case of point vortices ($\alpha = 0$) was studied by von Kármán (1912), see Lamb (1932, § 156). It was shown that infinitesimal two-dimensional disturbances of wavelength l/p grow like $e^{\sigma t}$, where

$$\frac{2l^2}{\pi\Gamma}\sigma = \pm B \pm (A^2 - C^2)^{\frac{1}{2}}, \tag{2.1}$$

$$A = 2p(1-p) - \operatorname{sech}^2 \pi\kappa, \tag{2.2}$$

$$B = i\left\{\frac{2p \sinh \pi\kappa(1-2p)}{\cosh \pi\kappa} + \frac{\sinh 2\pi\kappa p}{\cosh^2 \pi\kappa}\right\}, \tag{2.3}$$

$$C = \frac{\cosh 2\pi\kappa p}{\cosh^2 \pi\kappa} - \frac{2p \cosh \pi\kappa(1-2p)}{\cosh \pi\kappa}. \tag{2.4}$$

Note that p need not be an integer or rational. Since the steady flow has wavelength l, it follows from Floquet- or Bloch-wave theory that the normal modes of the system (for finite as well as point vortices) are of the form

$$e^{\sigma t} e^{2\pi x p/l} P(x, y), \tag{2.5}$$

where $P(x+l, y) \equiv P(x, y)$. Disturbances with p equal to an integer or zero will be called *superharmonic*; they always have wavelength l. If p is not equal to an integer, there is clearly no loss of generality in supposing that $0 < p < 1$, and such disturbances will in general have components with wavelengths greater than l and will be called *subharmonic*. Note that the properties of these disturbances (including the eigenvalue σ) must be the same for p and $1-p$, i.e. the problem exhibits symmetry in p about $p = 0.5$.

Figure 2 shows the regions of stable ($\mathscr{R}\sigma = 0$) and unstable ($\mathscr{R}\sigma > 0$) eigenfunctions in the (κ, p)-plane for point vortices. It should be noted that not all eigenfunctions are linearly unstable but for $\kappa \neq \kappa_c$ there always exist unstable disturbances. For $\kappa = \kappa_c$ (where $\cosh^2 \pi\kappa_c = 2$) all the disturbances are linearly stable, and this case was identified by von Kármán as the stable configuration of the street. However, it was discovered by Kochin (1939) that this 'stable' configuration is in fact unstable at second-order approximation in the disturbance amplitude (for an elegant demonstration, see Domm (1956)). These higher-order studies have dealt only with the case

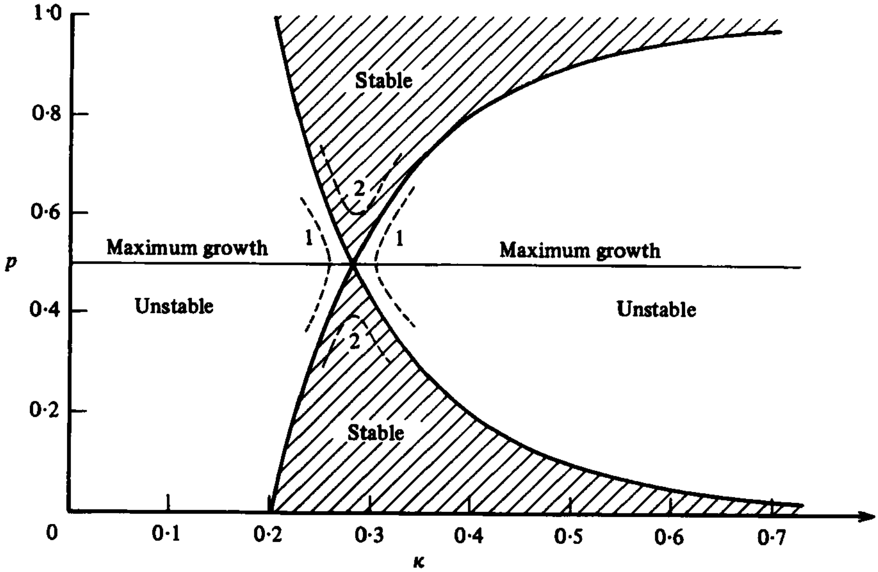

FIGURE 2. The stability boundary in the periodicity–spacing-ratio (p, κ)-plane for point-vortex configurations. The growth rates are symmetric about $p = 0.5$ which gives also the maximum rate of growth for all κ. Curves 1 and 2 show qualitatively the two possible perturbed boundaries for small area. The calculations indicate that curve 1 is the true result.

$p = 0.5$, and it is not known whether approximation of the evolution equations to order higher than first would lead to growing disturbances for other values of p. The disturbances for the $p = 0.5$, $\kappa = \kappa_c$ case grow in time as $e^{\epsilon t}$, where $\epsilon > 0$ is proportional to the initial disturbance, as opposed to the $e^{\sigma_R t}$ behaviour (σ_R independent of initial conditions) that occurs in the unstable region away from the stability/instability boundary.

Initially, it was hoped that an energy criterion could be used to answer this question of finite-amplitude stability away from the stability boundary. The Kirchhoff–Routh path function $W(x_1, y_1, x_2, y_2, \ldots)$ (which is a measure of the 'interaction energy', see Lin (1943)) determines the motion of the vortices (x_i, y_i) through the relations

$$\frac{dx_i}{dt} = -\frac{1}{\Gamma_i}\frac{\partial W}{\partial y_i}, \quad \frac{dy_i}{dt} = \frac{1}{\Gamma_i}\frac{\partial W}{\partial x_i}. \tag{2.6}$$

By a trivial change of variables, say $x_i \to -x_i$ for vortices with $\Gamma_i = -\Gamma$, this becomes a Hamiltonian system with Hamiltonian W. The right-hand sides of the (Hamilton's) equations may be expanded in Taylor series about the steady solutions x_i, y_i. The linearized equations reproduce figure 2. The second- and higher-order terms are, for sufficiently small deviation from the steady state, a small correction to the linear (and integrable) system. There exists a body of theory for such 'nearly integrable' Hamiltonian systems in the literature (see e.g. Chirikov 1979). In general, such systems exhibit the slow-instability phenomenon known as 'Arnol'd diffusion'. Fairly general bounds exist for the average growth rate of this instability (e.g. Nekhoroshev 1971) but these do not appear to provide useful conclusions for the present problem.

The stability boundaries of figure 2 will obviously be perturbed by the effect of finite size of the vortices, and the degenerate saddle will separate into one of the

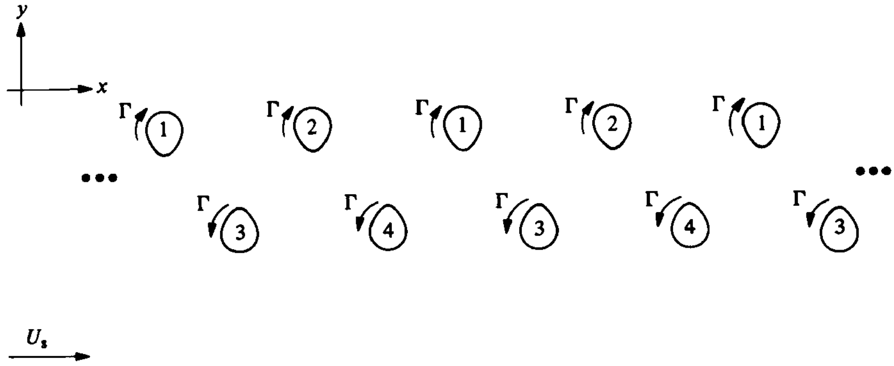

FIGURE 3. Diagram of the vortex-street configuration showing the four independent perturbations.

possibilities marked by the dashed lines in the figure. If case 1 is the situation, then there will be stability to infinitesimal disturbances for a finite range of κ in the vicinity of $\kappa = \kappa_c$. If case 2 obtains, then finite vortex size makes the array unstable for all κ. Remember that the symmetry about $p = 0{\cdot}5$ is valid for all α, so cases 1 and 2 are the only possibilities.

In principle, the problem of deciding between case 1 and case 2 can be treated by perturbation theory by expanding in powers of the area of the vortices, i.e. α. However, for reasons to be given below, it appears that the algebraic complexity is great, and direct numerical methods were employed instead. These, of course, have the advantage that they give results for finite areas not accessible to perturbation methods. In order to decide between case 1 and case 2, it clearly suffices because of the symmetry of figure 2 to consider only the subharmonic (pairing) disturbances with $p = 0{\cdot}5$, and we therefore restrict attention henceforth to disturbances that are periodic with period $2l$ in the x-direction. Of course, there is no guarantee that $p = 0{\cdot}5$ gives the maximum growth rate for finite α, so that the stability boundary for moderate and large α determined with $p = 0{\cdot}5$ may not be accurate. Note that the superharmonic disturbances are then automatically included, as these are trivially of period $2l$.

3. Analysis of the stability

It is appropriate for disturbances with period $2l$ to consider four independent perturbed vortex shapes (and positions), corresponding to the four vortices in one period $2l$, and extended periodically to infinity along the street, as in figure 3. The approach is to calculate the first variation of the velocity field due to a perturbation in vortex shape and position, and then to require that the linearized kinematic condition be satisfied on the boundaries of the vortices. In particular, solutions are looked for that are normal modes proportional to $e^{\sigma t}$; an eigenvalue problem is the result.

A convenient parametrization for the vortex boundaries is a polar co-ordinate representation

$$\left.\begin{aligned} z(\theta) &= z_0(\theta) + z'(\theta), \\ z'(\theta) &= \left[\tfrac{1}{2}\alpha_0 + \sum_{n=1}^{N} (a_n \cos n\theta + b_n \sin n\theta)\right] e^{i\theta}. \end{aligned}\right\} \tag{3.1}$$

Here $z_0(\theta)$ describes the steady boundary in question and $z'(\theta)$ describes the added disturbances.

As was shown previously (Saffman & Schatzman 1981), the complex velocity field produced by a single row of vortices (of spacing $2l$) can be calculated by integration around the boundary of a single vortex in the row as follows:

$$u+iv = \frac{\Gamma}{2\pi A}\int \log\left|\sin\frac{\pi}{l}(z-Z)\right| dZ, \tag{3.2}$$

where $z \equiv x+iy$ is the complex co-ordinate, lower-case variables refer to the point of evaluation of the flow field and capital variables refer to the path of integration. When evaluated on a vortex boundary, this will give the velocity contribution on the vortex boundaries of each vortex in the corresponding $2l$-periodic row due to disturbances of the other three $2l$-periodic vortex rows, added to the unperturbed value. Substituting $z = z_0+z'$, $Z = Z_0+Z'$, and assuming constant area A, the corresponding first variation of the velocity contribution is

$$u'+iv' = \frac{\Gamma}{2\pi A}\int\left[\log\left|\sin\frac{\pi}{2l}(z_0-Z_0)\right|\frac{dZ'}{d\Theta}+\mathscr{R}\left\{\frac{\pi}{2l}\cot\frac{\pi}{2l}(z_0-Z_0)(z'-Z')\right\}\frac{dZ_0}{d\Theta}\right]d\Theta. \tag{3.3}$$

As was remarked in the previous paper, the 'self-induced' velocity for one row of vortices may be written:

$$u+iv = \int\left[\left\{\log\left|\frac{\sin\frac{\pi}{2l}(z-Z)}{\frac{\pi}{2l}(z-Z)}\right| - i[\arg(z-Z)-\tfrac{1}{2}\Theta]\right\}\frac{dZ}{d\Theta}+\tfrac{1}{2}iZ\right]d\Theta - i\pi z, \tag{3.4}$$

where the arg function is taken so as to make the integrand periodic. The corresponding first variation is then:

$$\begin{aligned}u'+iv' = \frac{\Gamma}{2\pi A}\int\Bigg\{&\left[\mathscr{R}\left\{\left[\frac{\pi}{2l}\cot\frac{\pi}{2l}(z_0-Z_0)-\frac{1}{z_0-Z_0}\right](z'-Z')\right\}-\mathscr{I}\left(\frac{z'-Z'}{z_0-Z_0}\right)\right]\frac{dZ_0}{d\Theta}\\ &+\left[\log\left|\frac{\sin\frac{\pi}{2l}(z_0-Z_0)}{\frac{\pi}{2l}(z_0-Z_0)}\right| - i[\arg(z_0-Z_0)-\tfrac{1}{2}\Theta]\right]\frac{dZ'}{d\Theta}+\tfrac{1}{2}iZ'\Bigg\}d\Theta - i\pi z'.\end{aligned} \tag{3.5}$$

Note that all singularities of the integrand have been removed. To calculate the change in flow field due to the complete disturbance, three terms of the form (3.3) and one of the form (3.5) are summed with appropriate choice for the sign of Γ and the vortex co-ordinate parameters in each case.

The kinematic condition that the vortex boundaries move with the fluid may be written

$$\frac{D}{Dt}[r-R(\theta,t)] = 0. \tag{3.6}$$

Here

$$\left.\begin{aligned}R(\theta,t) &\equiv R_0(\theta)+R'(\theta,t),\\ \frac{D}{Dt} &\equiv \frac{\partial}{\partial t}+u_r\frac{\partial}{\partial r}+\frac{1}{r}u_\theta\frac{\partial}{\partial\theta},\end{aligned}\right\} \tag{3.7}$$

where, as before, the subscript zero refers to the unperturbed quantity and the prime refers to added perturbations. Also, u_r and u_θ are the polar velocity components. The solutions of interest are normal modes with perturbations proportional to $e^{\sigma t}$, so that

$$R'(\theta,t) = e^{\sigma t}R'(\theta), \quad u(r,\theta,t) = u_0(r,\theta)+e^{\sigma t}u'(r,\theta), \tag{3.8}$$

where the latter holds for each velocity component. To leading order

$$u(r,\theta) = \left[u_0+e^{\sigma t}\left(R'\frac{\partial u_0}{\partial r}+u'\right)\right](R_0,\theta) \tag{3.9}$$

for each velocity component. Equations (3.7)–(3.9) may be substituted into (3.6) and terms of second and higher order in the perturbation omitted, giving

$$u_r'+\frac{\partial u_{r0}}{\partial r}R'-\frac{1}{R_0}\frac{dR_0}{\partial\theta}\left(u_\theta'+\frac{\partial u_{\theta0}}{\partial r}R'\right) = \sigma R'\frac{1}{R_0^2}\frac{dR_0}{d\theta}u_{\theta0}R'+\frac{u_{\theta0}}{R_0}\frac{dR'}{d\theta}, \tag{3.10}$$

where now all quantities are evaluated on $r = R_0(\theta)$, and use has been made of the fact that

$$u_{r0}-\frac{1}{R_0}\frac{dR_0}{d\theta}u_{\theta0} = 0 \quad \text{on} \quad r = R_0. \tag{3.11}$$

The left-hand side of (3.10) is the perturbation in normal velocity component δu_n divided by the geometric factor

$$\cos\eta \equiv \left[1+\left(\frac{1}{R_0}\frac{dR_0}{d\theta}\right)^2\right]^{-\frac{1}{2}}, \tag{3.12}$$

where the effect of the change in normal direction due to the perturbation has been omitted. Also, $u_{\theta0}$ and the unperturbed tangential velocity component u_{t0} are related by

$$u_{\theta0} = u_{t0}\cos\eta, \tag{3.13}$$

so that (3.10) may be written

$$\delta u_n = \sigma\cos\eta R'-\cos^2\eta\frac{1}{R_0^2}\frac{dR_0}{d\theta}u_{t0}R'+\cos^2\eta\frac{u_{t0}}{R_0}\frac{dR'}{d\theta}. \tag{3.14}$$

This may be equated to the corresponding quantity calculated by the integration above (i.e. by (3.3) and (3.5)) and using

$$\left.\begin{aligned} \delta u_n &= \cos\eta\left(u_r'-\frac{1}{R_0}\frac{dR_0}{d\theta}u_\theta'\right), \\ u_r' = u'\cos\theta+v'\sin\theta, &\quad u_\theta' = -u'\sin\theta+v'\cos\theta. \end{aligned}\right\} \tag{3.15}$$

After substituting (3.1) and evaluating at the $2N+1$ points

$$\theta = \theta_j \equiv \frac{2\pi j}{2N+1} \quad (j = 0,1,\ldots,2N) \tag{3.16}$$

the result is a generalized eigenvalue problem of the form

$$\mathbf{A}\mathbf{w} = \sigma\mathbf{B}\mathbf{w}, \tag{3.17}$$

where **A** and **B** are $8N+4$ by $8N+4$ matrices and **w** is a vector containing the four sets of $2N+1$ Fourier coefficients from (3.1). The real parts of the eigenvalues of this system then give the growth rates of the corresponding normal modes. Inspection leads to the conclusion that, if σ is an eigenvalue, then so are $-\sigma$, σ^*, and $-\sigma^*$. Thus, it is evident that, at best, a steady state may have only normal modes with zero linear growth rate, and otherwise the state is linearly unstable.

For numerical purposes, the system (3.17) may be simplified somewhat by recognizing the symmetry of the problem. It is sufficient to consider disturbances where the vortex-shape perturbations z' are negative for vortices of rows 1 and 2 above, and similarly for rows 3 and 4. This simplification reduces the size of the system to $4N+2$ equations in two sets of Fourier coefficients. Values of N from 10 to 25 were used, depending on the size of the vortices.

Computations of the eigensystem were performed using the EIGZF subroutine in the IMSL library on an IBM 3032 computer (64 bit floating point). Some computational difficulties were encountered; an explanation follows. Note that, for isolated circular vortices of area A and circulation Γ, normal-mode perturbations exist of the form (see Lamb 1932, pp. 230–1)

$$R' = \epsilon \cos m\theta \, e^{\sigma t}, \quad \sigma = \tfrac{1}{2} i \frac{\Gamma}{2\pi A}(m-1) \quad (m = 2, 3, 4, \ldots). \tag{3.18}$$

Since the corresponding flow-field perturbations fall off in distance r as r^{-m-1}, and since small-area vortices for the street are nearly circular, it is evident that, for small A and large m, there will exist such solutions for the street. These in fact are the superharmonic disturbances. For small area A, these eigenvalues are much larger in modulus than the subharmonic ($p = 0{\cdot}5$) modes, which are bounded as A decreases. In fact, although this behaviour is most severe for small areas, for all states that were computed, these 'nearly isolated' modes had eigenvalues with dominating moduli. This characteristic showed itself in a great sensitivity of the calculated small eigenvalues to errors in the steady calculations (hence the matrices **A** and **B**). Typically, an error of roughly 0·1 % in radius or tangential velocity completely destroyed the small-eigenvalue computation. A second computational problem was failure of convergence of the iterative procedure for eigenvalue and eigenvector computation. This difficulty usually manifested itself near the stability/instability interface, and the explanation is not clear.

The results of the stability calculations are tabulated in table 1 and summarized in figure 4. Outside of the indicated region in the (κ, α)-plane, there are modes with positive growth rates, and hence these states are linearly unstable. Inside this region, there are no such modes (with x-period $2l$). With the exception of the smaller-energy state in the non-unique region, all eigenvalues corresponding to superharmonic disturbances were found to be purely imaginary. Aside from the trivial modes (uniform displacements) all non-growing modes are found to be given by (3.18) approximately with best matching for large m. There is agreement with the unsteady initial-value calculations of Christiansen & Zabusky (1973), as indicated in the figure. The superharmonic disturbances were always stable except for the smaller-energy solution in the non-unique region between curves 1 and 2.

For small areas, the width in κ of the stability region decreases and a plot of calculations in the vicinity (figure 5) indicates that the critical value of area α at which

κ	$\dfrac{A}{l^2}$	$\dfrac{l}{\Gamma}U_s$	$\dfrac{l}{\Gamma^2}T$	$\dfrac{l^2}{\Gamma}\lvert\sigma_R\rvert$	$\dfrac{l^2}{\Gamma}\lvert\sigma_I\rvert$
0·2	0	0·278447	∞	0·29825	0·72656
	0·49141(−3)	0·27845	0·58448	0·2983	0·7266
	0·43903(−1)	0·27586	0·22718	0·2996	0·7113
	0·69626(−1)	0·27204	0·19081	0·3003	0·6886
	0·93758(−1)	0·26704	0·16758	0·3000	0·6592
	0·13126	0·25709	0·14180	0·2959	0·5999
	0·18944	0·23839	0·11485	0·2732	0·4797
	0·26522	0·21281	0·43904(−1)	0·1007	0·2672
0·23	0	0·309248	∞	0·18451	0·76342
	0·78551(−4)	0·30925	0·73921	0·1845	0·7634
	0·54099(−1)	0·30609	0·21939	0·1890	0·7467
	0·11189	0·29933	0·17425	0·1961	0·6950
	0·16503	0·28125	0·13271	0·1948	0·6242
	0·19545	0·27142	0·12026	0·1882	0·5754
	0·23587	0·25755	0·10691	0·1603	0·4951
	0·29187	0·23803	0·92648(−1)	0·8594(−1)	0·5671
0·25	0	0·327897	∞	0·10985	0·77768
	0·78549(−4)	0·32790	0·74559	0·1099	0·7777
	0·57877(−1)	0·32490	0·22036	0·1154	0·7632
	0·99641(−1)	0·31889	0·17752	0·1201	0·7360
	0·10711	0·31748	0·17187	0·1204	0·7300
	0·11506	0·31587	0·16628	0·1202	0·7232
	0·19170	0·29544	0·12734	0·7787(−1)	0·6522
	0·20770	0·29032	0·12144	0·1709(−1)	0·6427
	0·22598	0·28425	0·11535	0	0·5304/0·7896
	0·24714	0·27700	0·10900	0·2075	0·7554
	0·27187	0·26835	0·10241	0·2384	0·6442
0·26	0	0·336666	∞	0·73237(−1)	0·78198
	0·12059	0·32466	0·16583	0·7640(−1)	0·7316
	0·15874	0·31581	0·14461	0·4205(−1)	0·7026
	0·16438	0·31432	0·14195	0·2596(−1)	0·6986
	0·17028	0·31273	0·13927	0	0·6688/0·7204
	0·21258	0·30011	0·12270	0	0·5357/0·8620
0·27	0	0·345072	∞	0·37231(−1)	0·78452
	0·78547(−4)	0·34507	0·75232	0·3723(−1)	0·7845
	0·52228(−1)	0·34315	0·23519	0·4078(−1)	0·7760
	0·11023	0·33612	0·17615	0·2624(−1)	0·7487
	0·11787	0·33479	0·17091	0·6564(−2)	0·7663
	0·12595	0·33328	0·16573	0	0·7162/0·7622
	0·20142	0·31468	0·12977	0	0·5489/0·8941
	0·21661	0·31012	0·12437	0·1387	0·1043(+1)
	0·23373	0·30473	0·11880	0·2870	0·9221
	0·25327	0·29833	0·11302	0·3419	0·8028
0·28054	0	0·353646	∞	0·34637(−4)	0·78540
	0·78546(−4)	0·35355	0·75600	0·3369(−4)	0·7854
	0·28358(−2)	0·35354	0·47061	0·3920(−4)	0·7854
	0·38640(−2)	0·35354	0·44599	0·2533(−4)	0·7854
	0·40889(−2)	0·35354	0·44148	0·1516(−4)	0·7854
	0·43203(−2)	0·35354	0·43710	0	0·7853/0·7854
	0·50531(−2)	0·35353	0·42464	0	0·7853/0·7854
0·280549	0	0·353553	∞	0·32318(−5)	0·78540
	0·78546(−4)	0·35355	0·75601	0·2047(−5)	0·7854
	0·70738(−3)	0·35355	0·58110	0·3719(−5)	0·7854

κ	$\dfrac{A}{l^2}$	$\dfrac{l}{\Gamma}U_s$	$\dfrac{l}{\Gamma^2}T$	$\dfrac{l^2}{\Gamma}\lvert\sigma_R\rvert$	$\dfrac{l^2}{\Gamma}\lvert\sigma_I\rvert$
	0·113 55(−2)	0·353 55	0·543 45	0·277 4(−5)	0·785 4
	0·125 83(−2)	0·353 55	0·535 27	0·132 7(−5)	0·785 4
	0·138 75(−2)	0·353 55	0·527 50	0	0·785 4/0·785 4
	0·283 58(−2)	0·353 55	0·470 61	0	0·785 4/0·785 4
0·280 549 926	0	0·353 553	∞	0	0·785 40
	0·785 46(−4)	0·353 55	0·756 01	0	0·785 40/0·785 40
	0·386 40(−2)	0·353 55	0·445 99	0	0·785 31/0·785 41
	0·261 45(−1)	0·353 15	0·293 86	0	0·781 2/0·786 0
	0·475 15(−1)	0·352 18	0·246 36	0	0·771 5/0·787 8
	0·765 62(−1)	0·349 88	0·208 52	0	0·748 7/0·792 6
	0·115 25	0·344 93	0·176 25	0	0·702 2/0·805 6
	0·204 68	0·325 24	0·131 94	0	0·540 6/0·991 7
	0·219 14	0·321 13	0·126 85	0·224 1	0·106 6(+1)
	0·235 27	0·316 30	0·121 60	0·333 4	0·952 5
	0·253 49	0·310 59	0·116 17	0·383 7	0·839 5
0·280 551	0	0·353 553	∞	0·374 71(−5)	0·785 40
	0·785 46(−4)	0·353 55	0·791 52	0·449 9(−5)	0·785 4
	0·616 15(−3)	0·353 55	0·592 09	0·261 7(−5)	0·785 4
	0·707 38(−3)	0·353 55	0·581 10	0·197 3(−5)	0·785 4
	0·804 93(−3)	0·353 55	0·570 82	0	0·785 4/0·785 4
	0·283 58(−2)	0·353 55	0·470 61	0	0·785 4/0·785 4
0·280 56	0	0·353 561	∞	0·351 52(−4)	0·785 40
	0·785 46(−4)	0·353 56	0·756 01	0·362 2(−4)	0·785 4
	0·707 38(−3)	0·353 56	0·581 11	0·341 2(−4)	0·785 4
	0·212 85(−2)	0·353 56	0·493 45	0·197 0(−4)	0·785 4
	0·229 57(−2)	0·353 56	0·487 43	0·143 3(−4)	0·785 4
	0·246 94(−2)	0·353 56	0·481 62	0	0·785 4/0·785 4
	0·505 31(−2)	0·353 55	0·424 64	0	0·785 2/0·785 4
0·29	0	0·360 821	∞	0·326 20(−1)	0·784 72
	0·785 46(−4)	0·360 82	0·759 38	0·326 2(−1)	0·784 7
	0·357 69(−1)	0·360 16	0·272 30	0·301 2(−1)	0·782 0
	0·703 86(−1)	0·358 14	0·218 53	0·155 9(−1)	0·774 4
	0·756 98(−1)	0·357 70	0·212 71	0·742 0(−2)	0·772 9
	0·812 53(−1)	0·357 21	0·207 15	0	0·757 8/0·784 5
	0·128 07	0·351 35	0·171 27	0	0·686 7/0·822 2
	0·208 41	0·334 37	0·133 70	0	0·539 5/0·110 9(+1)
	0·222 27	0·330 65	0·128 87	0·275 2	0·107 7(+1)
	0·254 75	0·321 19	0·118 80	0·414 9	0·865 1
0·3	0	0·368 179	∞	0·663 25(−1)	0·782 59
	0·491 06(−3)	0·368 18	0·617 17	0·663 0(−1)	0·782 6
	0·802 51(−1)	0·365 19	0·211 75	0·523 6(−1)	0·772 1
	0·104 34	0·362 95	0·109 98	0·307 1(−1)	0·765 6
	0·111 02	0·362 20	0·186 08	0·148 0(−1)	0·763 7
	0·118 00	0·361 36	0·181 27	0	0·735 8/0·787 8
	0·149 29	0·356 83	0·162 83	0	0·669 9/0·839 6
	0·198 94	0·347 08	0·140 64	0	0·573 9/0·991 9
	0·210 98	0·344 27	0·136 17	0·952 8(−1)	0·119 5(+1)
	0·224 04	0·341 04	0·131 63	0·297 8	0·109 7(+1)
	0·254 13	0·332 92	0·122 25	0·440 1	0·903 0
0·31	0	0·375 205	∞	0·991 42(−1)	0·779 12
	0·785 44(−4)	0·375 21	0·766 75	0·991 4(−1)	0·779 1
	0·506 67(−1)	0·374 27	0·251 96	0·956 8(−1)	0·775 8

κ	$\frac{A}{l^2}$	$\frac{l}{\Gamma}U_s$	$\frac{l}{\Gamma^2}T$	$\frac{l^2}{\Gamma}\lvert\sigma_R\rvert$	$\frac{l^2}{\Gamma}\lvert\sigma_I\rvert$
	0·12276	0·36896	0·18181	0·6074(−1)	0·7624
	0·13757	0·36718	0·17285	0·3000(−1)	0·7600
	0·14546	0·36613	0·16848	0	0·7270/0·7915
	0·20165	0·35651	0·14312	0	0·5917/0·1003(+1)
	0·23845	0·34827	0·13039	0·3926	0·1030(+1)
	0·25286	0·34466	0·12600	0·4485	0·9418
0·32	0	0·381908	∞	0·1310	0·7744
	0·14979	0·37391	0·16988	0·7580(−1)	0·7607
	0·16285	0·37224	0·16333	0·1929(−1)	0·7357
	0·16972	0·37129	0·16010	0	0·7259/0·8019
	0·21245	0·36426	0·14273	0	0·6011/0·1101(+1)
	0·23075	0·36066	0·13642	0·3310	0·1107(+1)
0·33	0	0·388296	∞	0·16194	0·76852
	0·78542(−4)	0·38830	0·77438	0·1619	0·7685
	0·11194	0·38503	0·19664	0·1495	0·7610
	0·16992	0·37975	0·16377	0·1016	0·7639
	0·18717	0·37759	0·15623	0·7995(−1)	0·7634
	0·19633	0·37633	0·15252	0	0·7078/0·8606
	0·21589	0·37337	0·14518	0	0·6398/0·1061(+1)
	0·22640	0·37164	0·14153	0·2403	0·1153(+1)
	0·24924	0·36751	0·13421	0·4310	0·1016(+1)
	0·30562	0·35523	0·11902	0·5504	0·7343
0·34	0	0·394380	∞	0·19186	0·76160
	0·18987	0·38583	0·15893	0·1304	0·7724
	0·20391	0·38423	0·15338	0·8383(−1)	0·7898
	0·21124	0·38334	0·15065	0	0·7724/0·8392
	0·22265	0·38187	0·14658	0	0·6925/0·1040(+1)
	0·22658	0·38134	0·14524	0·1254	0·1156(+1)
	0·23463	0·38022	0·14256	0·2827	0·1112(+1)
0·35	0	0·400170	∞	0·22077	0·75373
	0·78541(−4)	0·40017	0·78227	0·2208	0·7537
	0·76127(−1)	0·39951	0·23509	0·2195	0·7522
	0·20899	0·20899	0·39237	0·1911	0·7859
	0·23583	0·38972	0·14601	0·1738	0·1088(+1)
	0·24533	0·38868	0·14298	0·1708(−1)	0·1174(+1)
	0·25515	0·38756	0·13998	0·4067	0·1008(+1)
	0·27583	0·38505	0·13407	0·5091	0·9151
0·4	0	0·425067	∞	0·34986	0·70317
	0·78319(−2)	0·42508	0·43669	0·3499	0·7032
	0·68688(−1)	0·42557	0·26392	0·3542	0·7039
	0·17769	0·42792	0·18863	0·3913	0·7074
	0·28875	0·43949	0·15123	0·5747	0·6924
	0·30799	0·45558	0·14654	0·7112	0·6083
	0·29328	0·47296	0·14969	0·3436	0·5366
0·5	0	0·458576	∞	0·53591	0·57415
	0·77869(−2)	0·45859	0·48149	0·5360	0·5742
	0·65486(−1)	0·45962	0·31214	0·5448	0·5734
	0·15776	0·46487	0·24282	0·5958	0·5623
	0·24031	0·47659	0·21092	0·7247	0·5115
	0·26263	0·48525	0·20473	0·8446	0·4515
	0·26361	0·48779	0·20449	0·8971	0·4221
	0·26285	0·48892	0·20467	0·9293	0·4003

Note: Numbers in parentheses indicate powers of 10 that multiply the preceding mantissas.

TABLE 1

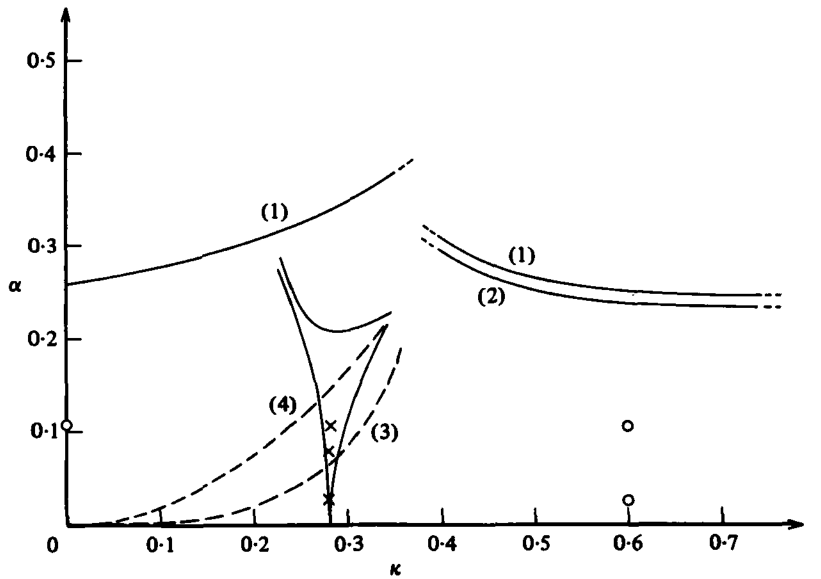

FIGURE 4. A plot of the area-spacing-ratio (α, κ)-plane. Curve 1 denotes the maximum area for a given spacing ratio. The segment corresponding to smaller κ should be regarded as a lower bound for the maximum area because slow convergence in this region made it difficult to find the precise α at which vortices touched. Above curve 2, there are two solutions for a given pair (α, κ). The enclosed central region has neutral linear stability; configurations outside this region are linearly unstable. Curve 3 (see §4) shows the line $E_2 = E_3$, below and to the right $E_2 > E_3$. Curve 4 shows the largest area for which configuration (2) exists. The symbols × mark stable and ○ mark unstable states according to Christiansen & Zabusky (1973).

stabilization occurs, asymptotically for small area, is approximately

$$\left.\begin{aligned}\alpha &\simeq 1{\cdot}31(\kappa_c-\kappa)^{\frac{1}{2}} \quad (\kappa < \kappa_c),\\ \alpha &\simeq 0{\cdot}78(\kappa-\kappa_c)^{\frac{1}{2}} \quad (\kappa > \kappa_c).\end{aligned}\right\} \tag{3.19}$$

This approximate result indicates for the following reason that its exact calculation by perturbation analysis may be a laborious task. When $\alpha = 0$ and $p = 0{\cdot}5$, the eigenvalues are the roots of the quartic

$$\sigma^4 + 2(B^2 - A^2)\,\sigma^2 + (B^2 + A^2)^2 = 0. \tag{3.20}$$

It is expected that the coefficients of the equation for the eigenvalues are analytic functions of κ and α. Hence, for $\alpha \ll 1$, the perturbed eigenvalues are roots of the quartic

$$\sigma^4 + [(2(B^2 - A^2) + \alpha^2 f_2(\kappa) + \alpha^4 f_4(\kappa) + \dots]\,\sigma^2 + [(B^2 + A^2)^2 + \alpha^2 g_2(\kappa) + \alpha^4 g_4(\kappa) + \dots] = 0. \tag{3.21}$$

(Invariance to changes in the sign of the vorticity requires the coefficients to be even functions of α.) The roots will, as functions of α, have branch-point singularities, corresponding to a change in stability of the system, where the roots of the quartic are not distinct, i.e. when

$$-16A^2B^2 + [4(B^2 - A^2)f_2 - 4g_2]\,\alpha^2 + [4(B^2 - A^2)f_4 + f_2^2 - 4g_4]\,\alpha^4 + \dots = 0. \tag{3.22}$$

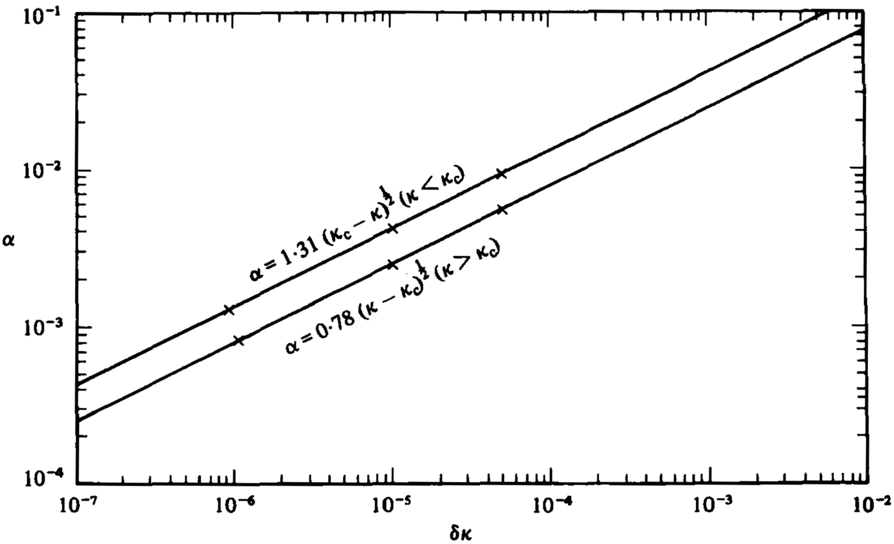

FIGURE 5. A logarithmic plot of the critical area α at which stabilization occurs versus the distance in κ away from $\kappa_c = 0{\cdot}280\,549\,926\ldots$.

The results shown in figure 5 indicate that, when expanded in $\kappa - \kappa_c$ as well as α, this equation takes the approximate form

$$1{\cdot}04(\kappa - \kappa_c)^2 - 2{\cdot}32\alpha^2(\kappa - \kappa_c) + \alpha^4 = 0. \tag{3.23}$$

The principal point, however, is that it is necessary to go to fourth order in α in order to determine the behaviour of the eigenvalues for small area.

4. The energy criterion for stability

It was pointed out by Kelvin (1910, p. 116) (see also Arnol'd 1980, p. 335) that, for given vorticity and momentum, steady states correspond to stationary points of the kinetic energy with respect to kinematically allowable isovortical perturbations. The steady state is then stable if it is a local maximum or minimum in energy.

For this problem, assuming perturbations periodic in the streamwise direction (say with period Nl, N an integer), it is sufficient to apply the above criterion to one period of the flow field. Holding the vorticity constant, and assuming that vortices of opposite sense do not amalgamate, the requirement of kinematically allowable perturbations forces the total area of the vortices of each sense to remain unchanged. The condition of momentum invariance requires that the components of hydrodynamic impulse per unit length,

$$I_x = -\frac{1}{Nl}\int_0^{Nl}\int_{-\infty}^{+\infty} \omega y\, dx\, dy = \frac{\Gamma h}{l}, \tag{4.1}$$

$$I_y = -\frac{1}{Nl}\int_0^{Nl}\int_{-\infty}^{+\infty} \omega x\, dx\, dy = 0. \tag{4.2}$$

stay constant. This is ensured by keeping the distance between the centroids of the two rows constant. In the following discussion it will be assumed that $N = 2$.

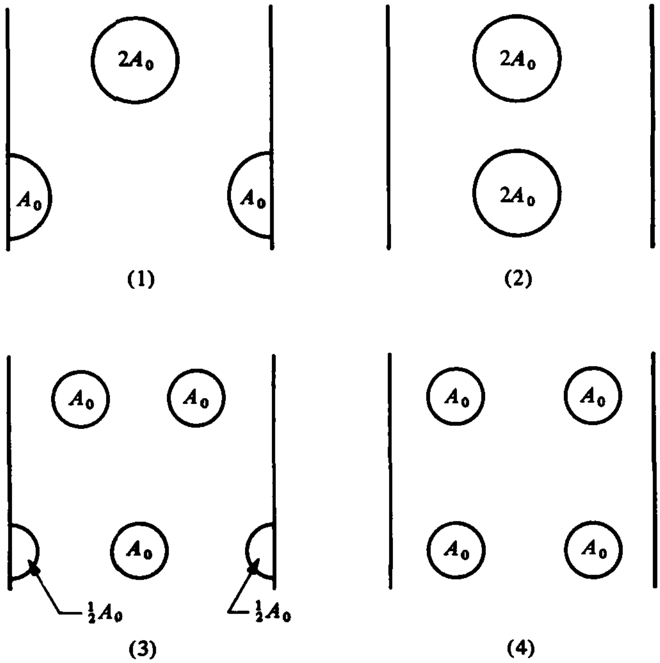

FIGURE 6. The four vortex configurations for the energy criterion for stability.

Now consider a system with period $2l_0$ and consider the following four configurations (see figure 6):

$$\left.\begin{array}{lllll}(1) & l = 2l_0, & d = l_0, & h = h_0, & A = 2A_0; \\ (2) & l = 2l_0, & d = 0, & h = h_0, & A = 2A_0; \\ (3) & l = l_0, & d = \frac{1}{2}l_0, & h = h_0, & A = A_0; \\ (4) & l = l_0, & d = 0, & h = h_0, & A = A_0. \end{array}\right\} \tag{4.3}$$

These states are apparently unique for small values of α (below curve 2 in figure 4 for states (1) and (3)). It is clear that these four states satisfy the above conditions (4.1) and (4.2). Presumably, there are other steady states that do so, such as finer splittings and multiple-vortex layers, but the existence of such configurations is not crucial to this argument, as their energy is believed to be less than that of configuration (4) because of the general consideration that spreading out the vorticity of one sign and mixing the vorticity of opposite signs reduces the energy (Onsager 1949). We are concerned with the stability of configuration (3) to superharmonic disturbances of period l_0 in which all vortices in a row are disturbed in the same way, and to subharmonic disturbances of period $2l_0$.

Calculations based on the circular-vortex approximation (Saffman & Schatzman 1981) indicate that the energies of the four steady states can be ranked as follows when $\alpha = A_0/l_0^2$ is small:

$$E_1 > E_2 > E_3 > E_4. \tag{4.4}$$

Since E is clearly bounded above, E_1 is an absolute maximum (since otherwise there would have to be another steady state with the same periodicity and greater energy) and configuration (1) is stable; it follows from the similarity of (1) and (3) that configuration (3) is stable to all *superharmonic* disturbances, and this will remain true for all α below curve 2 in figure 3. (When there are two states, the one with less energy will be unstable.) This confirms our calculations of *superharmonic* instability but state (3) is not stable to *subharmonic* disturbances for κ outside the range shown in figure 4 and will therefore be in this range a minimax of energy.

Now it can be shown from calculations of the system with $d = 0$ that when α is large it is possible for $E_2 < E_3$ to occur. When this problem was first studied, it was speculated that a mechanism for the stabilization of configuration (3) against subharmonic infinitesimal and finite-amplitude disturbances is that the drop in E_2 below E_3 for sufficiently large area results in a change in the topology of the energy surface in the infinite-dimensional configuration space (for this configuration) so that it becomes a local maximum in energy. Non-dimensionalization leads to $T = l^{-1}\Gamma^2\hat{T}(\alpha, \kappa, \mu)$ for the energy per unit length of a given steady state (assuming it exists). The condition that $E_2 = E_3$ then leads to:

$$2\hat{T}(\tfrac{1}{2}\alpha, \tfrac{1}{2}\kappa, 0) = \hat{T}(\alpha, \kappa, \tfrac{1}{2}), \tag{4.5}$$

where α and κ are the parameters associated with configuration (3). The result of applying this criterion is shown by curve 3 of figure 4. It was observed that for the $\mu = 0$ cases (configurations (2) and (4)), solutions exist only for vortices up to a limiting area. As the vortex area approaches this limit adjacent vortices in opposite rows approach each other. It is believed that this behaviour is qualitatively similar to that observed for a pair of counter-rotating vortices by Pierrehumbert (1980). For small κ, the limit occurs at small area, and, since interactions between neighbouring pairs are then small, the counter-rotating vortex pair should indeed be a good approximation. Curve 4 of figure 4 represents this approximation. Some calculations for the exact problem were attempted and are in reasonable agreement with curve 4 (the approximate calculated limiting areas were always less than curve 4 and within about 25 %). However, accurate calculation of the limiting area is prohibitively expensive, and was not undertaken. According to this argument, the region of stability lies between curves 3 and 4 in figure 4 and is moreover a region of stability to finite-amplitude disturbances that are not too large. The results of the linear stability analysis shows that this argument is fallacious. Incidentally, there is no evidence to suggest that the symmetrical configuration ($d = 0$) can be stabilized by finite size, but Taneda (1965) reported that oscillation of the body produced streets of symmetrical vortices. We can offer at present no explanation of this phenomenon.

5. Conclusion

We have generalized von Kármán's analysis of the linear stability of the point-vortex street to vortices of finite size and demonstrated that finite size can stabilize the array. The boundary of the linear-stability region for subharmonic disturbances of period twice the separation is shown in figure 4. The open questions deal with nonlinear stability and with stability to more general disturbances. At present, there seems to be no way to study the former question other than by direct numerical calculation of an initial-value problem. This was carried out to some approximation by Christiansen & Zabusky (1973), as commented earlier, and their results indicate that linear stability implies nonlinear stability or, at least, very slow growth. The possibility of unstable disturbances of more general character than those considered here could also be investigated in this way.

For point vortices, the equations of motion amount to a Hamiltonian system of a finite number of degrees of freedom (depending on the assumed periodicity) and the theory of nearly integrable systems (e.g. see Chirikov 1979) suggests that this system is subject to slow instability ('Arnol'd diffusion'). However, it may be that the instability is so slow that streets of physical interest are in a practical sense stable. This question has not been resolved. Intuitively, one can perhaps expect this behaviour to persist to the finite-area case, but it would be worth while to investigate this matter further.

The importance of studying the stability to three-dimensional disturbances goes without saying, but this is a difficult problem at present.

This work was supported by the Department of Energy (Office of Basic Energy Sciences). We acknowledge with gratitude the granting of time by Control Data Corporation on the CYBER 203 computer at the C.D.C. Service Center, Arden Hills, Minnesota, where much of the more difficult computing was carried out.

REFERENCES

ARNOL'D, V. I. 1980 *Mathematical Methods of Classical Mechanics*, pp. 332–337. Springer.

CHIRIKOV, B. V. 1979 A universal instability of many-dimensional oscillator systems. *Phys. Rep.* **52**, 263–379.

CHRISTIANSEN, J. P. & ZABUSKY, N. J. 1973 Instability, coalescence and fission of finite-area vortex structures. *J. Fluid Mech.* **61**, 219–243.

DOMM, U. 1956 Über die Wirbelstraßen von geringster Instabilität. *Z. angew. Math. Mech.* **30**, 367–371.

VON KÁRMÁN, T. 1912 Über den Mechanismus des Widerstands, den ein bewegter Körper in einer Flüssigkeit erfährt. *Gött. Nachr. Math. Phys. Kl.* **00**, 547–556.

KELVIN, LORD 1910 *Mathematical and Physical Papers*, vol. IV. Cambridge University Press.

KOCHIN, N. J. 1939 On the instability of von Kármán's vortex street. *C. R. Acad. Sci. U.R.S.S.* **24**, 19–23.

LAMB, H. 1932 *Hydrodynamics*, 6th edn. Cambridge University Press.

LIN, C. C. 1943 On the motion of vortices in two dimensions. *University of Toronto Studies, Appl. Math. Series*, vol. 5.

ONSAGER, L. 1949 Statistical hydrodynamics. *Suppl. Nuovo Cim.* **6**, 279–287.

NEKHOROSHEV, N. N. 1971 The behaviour of Hamiltonian systems that are close to integrable. *Func. Anal. Appl.* **5**, 338–339.

PIERREHUMBERT, R. T. 1980 A family of steady, translating vortex pairs with distributed vorticity. *J. Fluid Mech.* **99**, 129–144.

ROSENHEAD, L. 1929 Double row of vortices with arbitrary stagger. *Proc. Camb. Phil. Soc.* **25**, 132–138.

SAFFMAN, P. G. & SCHATZMAN, J. C. 1981 Properties of a vortex street of finite vortices. *SIAM J. Sci. Stat. Comp.* (to be published).

TANEDA, S. 1965 Experimental investigation of vortex streets. *J. Phys. Soc. Japan* **20**, 1714–1721.